

# HORIZONTAL TESTING AND THERMAL CYCLING OF AN N-DOPED TESLA TYPE CAVITY

O. Kugeler, J. Köszegei, J. Knobloch, Helmholtz Zentrum Berlin, Germany  
A. Grassellino, O. Melnychuk, A. Romanenko, D. Sergatskov, Fermilab, USA

## Abstract

An N-doped TESLA type cavity treated at FERMILAB has been tested in the HoBiCaT horizontal test stand. Temperatures and magnetic fields occurring during the superconducting transition were recorded at various positions and directions on the outer cavity surface. Several thermal cycling runs were performed yielding different  $Q_0$  factors just like in undoped cavities. The resulting residual and BCS resistance values were correlated to the thermal and magnetic conditions during cooldown and compared to values obtained in a vertical test at Fermilab.

## INTRODUCTION

In the strife for maximizing  $Q_0$  of superconducting Nb cavities, two technical developments have led to major advances in the past few years: The controlled contamination of the material by N-doping [1] and the optimization of magnetic flux expulsion by thermal cycling [2]. The amount of trapped flux is given by the total amount of ambient flux in the instance of the superconducting transition [3] and the efficiency of the expulsion driven by the Meissner effect [4-6].

The total ambient flux is given by the fraction of the Earth magnetic field that is not removed by the magnetic shielding (typically  $<1\%$  or  $<0.5 \mu\text{T}$ ) plus a contribution due to thermal currents [7]. Thermal currents occur when conducting loops of different materials with different Seebeck coefficients (Nb, Ti, NbTi, ...) exist in the cavity-tank system and these loops are subject to a superimposed temperature profile.

The efficiency of the Meissner expulsion is correlated to the temperature gradients in the instance of the transition. While in conduction cooled model systems a small gradient leads to better expulsion and reduced trapped flux [8] the opposite is observed in vertical cavity tests, where faster cooling through  $T_c$  results in larger quality factors [5]. The dependence of the obtained  $Q_0$  factor on the cooling gradient can even be different for horizontal and vertical tests. In order to extract which observations might be due to systematic influence of the testing environment and which measurements from the cavity by itself, a joint effort has been established to test one particular cavity in different cryostats at different labs. The measurements presented here have been done at the horizontal test facility at HZB, HoBiCaT [9]. Previous measurements were done horizontally at Cornell [10] and vertically with and without tank at Fermilab.

## EXPERIMENTAL SETUP

All measurements have been performed on the TB9AES11 cavity, a TESLA type cavity that was N-doped with the standard Fermilab recipe [1]. The cavity was encased in a magnetic shielding, a second magnetic shield was present the inside wall of the HoBiCaT cryostat. Fluxgate magnetic field sensors were attached at the cavity walls at different positions and with different orientations: Fluxgate FG1, FG3 and FG4 were placed radially on the outer and middle cells parallel to the cavity surface near the equator, to monitor the Meissner transition. FG2 was placed azimuthally on one of the outer cells in order to observe thermal currents due to the toroidal current loop formed by cavity (Nb) and tank (Ti). Cernox temperature sensors CX7, CX8, and CX5 were placed on top of the outer cells and the middle cell in order to measure temperature differences in axial direction of the cavity, CX6 was placed at the bottom of an outer cell which in combination with CX5 allowed for the measurement of a vertical temperature difference

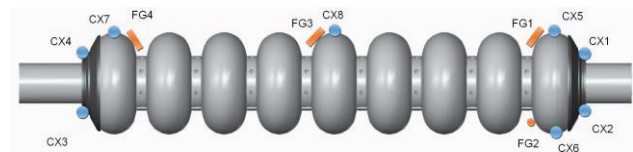


Figure 1: Positions and orientations of CERNOX temperature sensors and Fluxgate magnetometers on the TB9AES11 cavity.

across one cell. The beam pipe and the outer helium vessel were equipped with further CERNOX temperature sensors CX1 and CX2 on the input coupler side and CX3 and CX4 on the other side. All measured values were recorded with a Labview and EPICS system on a one second basis. Heaters were attached at both beam pipes in order impose temperature gradients during cool down. The cavity was equipped with a near critically coupled fixed, low-power input antenna. The resulting high loaded  $Q_L > 1 \cdot 10^{10}$  allowed for precise measurement of the high expected  $Q_0$  values. The pickup probe had an external  $Q$  of ca.  $1 \cdot 10^{12}$ . RF operation of the cavity was performed with a PLL. Due to the HoBiCaT infrastructure the RF drive signal was amplified with a 15 kW Bruker solid state amp, passed through a 17 m of HCA300-50J flexible coaxial cable, then through a WR-650 waveguide with circulator and three-stub-tuner. From there it was adapted to N type connector and LMR-400 cable and connected to a feedthrough at the cryostat. Inside the vacuum it was further adapted to SMA connectors and Huber+Suhner K\_03252\_D-06 cable.

Forward power and reflected power were extracted before the cryostat with a NARDA 20dB directional coupler and measured with a Gigatronics 8542C and CW power heads. The transmitted power was measured directly with a Gigatronics 8541C. Beta values were obtained from the pulse pattern of the reflected power observed on a fast oscilloscope and - for comparison and redundancy - from the equilibrium power levels of forward, reflected and transmitted power at CW mode.

The cavity has been subjected to a variety of thermal cycling runs, each one leading to a temporary transition to the fully normal conducting state and thus a redistribution or a different total amount of trapped flux in the cavity wall upon renewed transition through  $T_c$ . Temperature profiles were varied by using heaters attached to the ends of the cavity and manually controlling the Helium flow into the cryostat. After each cycle a  $Q_0$  vs  $E_{acc}$  curve was taken for the  $\pi$  mode and the  $8/9 \pi$  mode of the cavity. The  $8/9 \pi$  mode has more field in the outer cells and allows for the detection of non-uniformly distributed trapped flux. The  $1/9 \pi$  mode has a higher field in the inner cells and thus delivers complimentary information. However, the coupling of the pickup antenna was too weak to resolve the  $1/9 \pi$  mode, it could therefore not be measured in the setup presented here.

### RESULTS

Similar to measurements at undoped cavities and the horizontal tests at Cornell [10] the obtained  $Q_0$  values spread over a wide range depending on the cool down conditions. Figure 2 shows an overview of all data points taken after all of the thermal cycling runs.

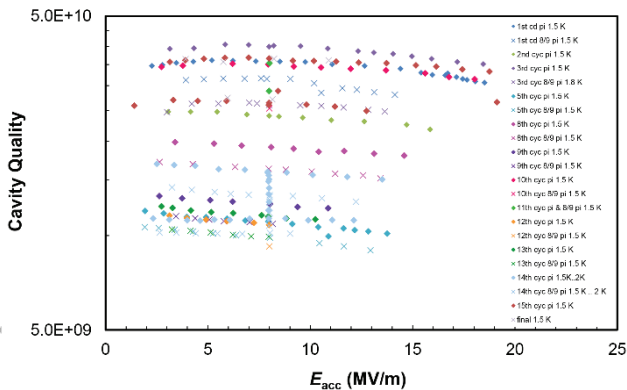


Figure 2: Overview of  $Q_0$  vs  $E_{acc}$  curves taken after thermal cycles. For better comparability the  $8/9\pi$  mode has been scaled with the same R/Q value as the  $\pi$  mode. Temperatures were 1.5 K unless otherwise stated.

The maximum obtained accelerating gradient was 19 MV/m. We observe a marginal negative Q-slope only at lowest temperature (1.5 K, upper graphs) and below 10 MV/m. Performance was limited by heating of the RF

cable which occurred at forward power levels larger than 10 W.

Figure 3: shows temperatures and magnetic fields during initial cool down. There are two peculiarities in the recorded data: (1) the temperatures measured at the surface of the cavity cells do not lag behind the temperatures measured at the beam pipe outside the tank significantly; the superconducting transition occurs only a little earlier than one would assume when only looking at the outside temperatures. (2) the azimuthally attached fluxgate probe FG2 that is most sensitive to magnetic fields due to thermal currents shows a large value of more

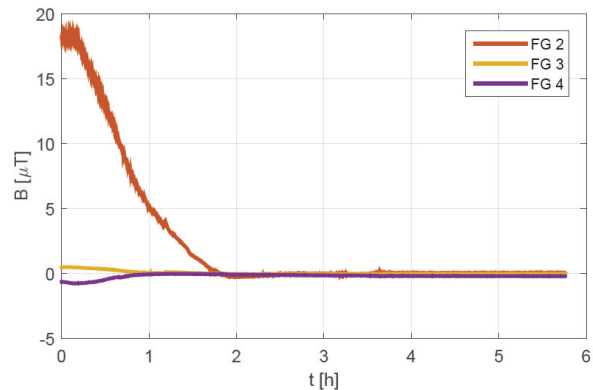
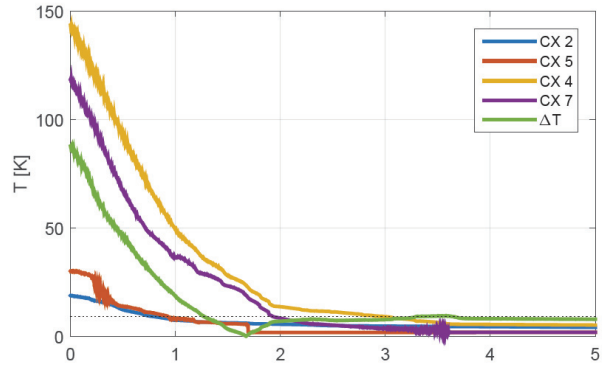


Figure 3: Temperatures and magnetic fields during initial cool down.

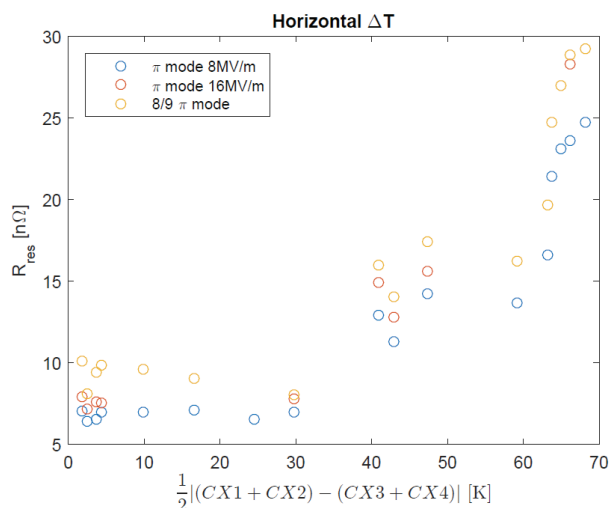


Figure 4: Residual resistance extracted from the measured  $Q_0$  data at different axial temperature gradients at the transition through  $T_c$ .

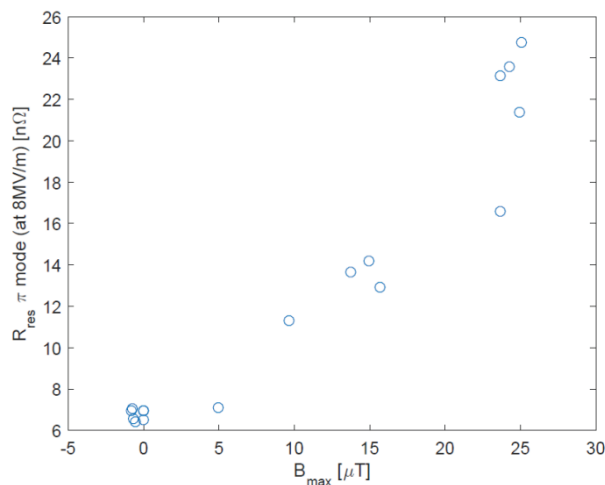


Figure 5: Residual resistance as a function of the maximum B field induced by thermal currents.

than 7  $\mu\text{T}$  at the superconducting transition.

In the subsequent thermal cycling runs it was attempted by adjusting the heater power appropriately to disentangle the contributions of horizontal (axial) temperature gradient, vertical temperature gradient and thermal current on the trapped flux. Figure 4 shows the residual resistance extracted from the measured  $Q_0$  data points at 8 MV/m and 16 MV/m and the values obtained for the 8/9  $\pi$  mode at a field gradient corresponding to 8 MV/m for different axial temperature differences. There is a slight decrease of the residual resistance with temperature difference for  $\Delta T < 30\text{K}$  which corresponds to the observation in vertical tests of decreasing residual resistance with cool down speed. Above  $\Delta T = 30\text{K}$  we observe a strong increase of residual resistance which we interpret as the onset of thermal currents. The 8/9  $\pi$  mode shows an elevated residual resistance by  $\sim 3\text{ n}\Omega$  throughout all temperature differences besides the minimum at 30 K which means that the expulsion efficiency is not improved (or diminished) at the outer cells. A discrepancy here would have hinted against the significance of thermal currents on the trapped flux, since the thermal currents are the same along the cavity axis while a magnetic shielding works better at the inside cells. In Figure 5 the residual resistance in the  $\pi$  mode at 8 MV/m is plotted against the measured magnetic field  $B_{\text{max}}$  in the azimuthal fluxgate FG2.

All cool down curves exhibit a spike  $B_{\text{max}}$  in the magnetic field, as exemplarily shown in Figure 6. The spike is very likely caused by the spontaneous discontinuous transition of the Seebeck coefficient from  $S < 0$  in normal conducting state to  $S = 0$  in superconducting state. While this spike does not necessarily reflect the amount of field that is trapped in the cavity, it serves as a good reference point for comparison with other thermal cycles.

Figure 5 shows a very strong correlation between the extracted residual resistance and the peak magnetic field due to Seebeck effect. It would be premature, however, to attempt to extract quantitative data from this measurement – a more thorough measurement of the magnetic field would be required for this.

The discontinuity of the Seebeck coefficient is smeared out over time because not all parts of the cavity are making the transition simultaneously, therefore the width of the spread is a measure for the effective cooling gradient, independent of temperature measurements. In an additional attempt at evaluating the thermal cycling data, the extracted residual resistance was plotted against the temperature difference across one cell (i.e. in the vertical direction in a horizontal test), see Figure 7. The results suggest that a small temperature gradient in the vertical direction is advantageous and leads to smaller residual resistances.

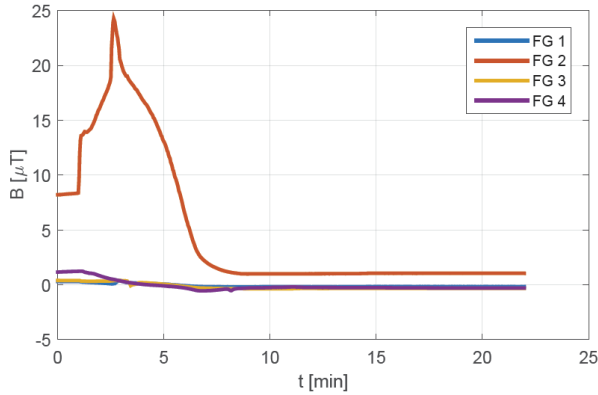
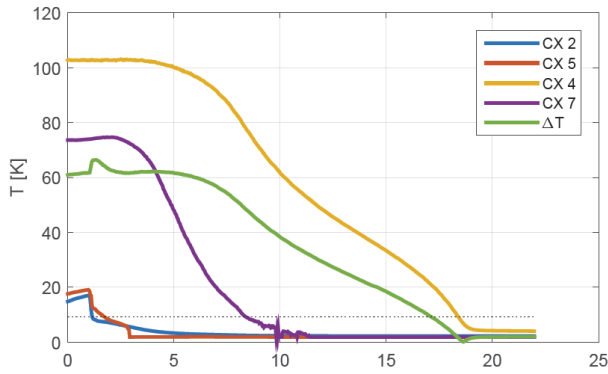


Figure 6: Temperature profile and magnetic flux during typical thermal cycling run. The spike coincides with the superconducting transition process of the cavity.

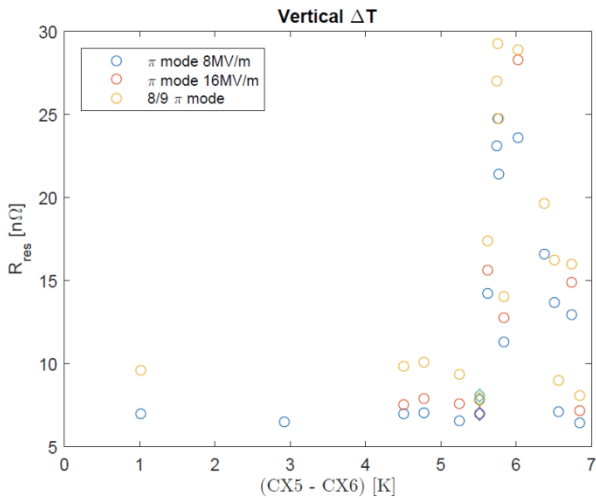


Figure 7: Residual resistance obtained for varying temperature differences between top and bottom of a cell.

### CONCLUSION

Horizontal testing of the N-doped Fermilab TB9AES11 cavity at HZB yielded slightly reduced  $Q_0$  values and similar  $E_{acc}$  values compared to measurements done with the same cavity vertically at Fermilab and horizontally at Cornell. Magnetic fields due to thermal currents could be directly measured and played a role at temperature differences larger than 30 K.

### ACKNOWLEDGMENT

We would like to thank André Frahm, Michael Schuster, Sascha Klauke, Stefan Rotterdam and Dirk Pflückhahn for support in setting up the experiment.

### REFERENCES

- [1] Grassellino, A. et al. *Superconductor Science and Technology*, 26(10), 102001.
- [2] Vogt, J.-M., et al. *Physical Review Special Topics - Accelerators and Beams*, 16(10), 102002.
- [3] Padamsee, H. et al. *RF Superconductivity for Accelerators 2<sup>nd</sup> ed.*, Wiley (2008).
- [4] Kugeler, O. et al. *Proc. IPAC 2012*.
- [5] Romanenko, A, et al. *J. Appl. Phys.*, 115, 184903.
- [6] Martinello, M. et al. *Journal of Applied Physics*, 118(4), 044505.
- [7] Vogt, J. et al. *PRSTAB* 18 042001 (2015).
- [8] Vogt, J. Master thesis (2013) Humboldt Universität Berlin.
- [9] Kugeler, O. et al, *Review of Scientific Instruments*, 81(7), (2010).
- [10] Gonnella, D. et al, *J. Appl. Phys.*, 117(203908)(2015).